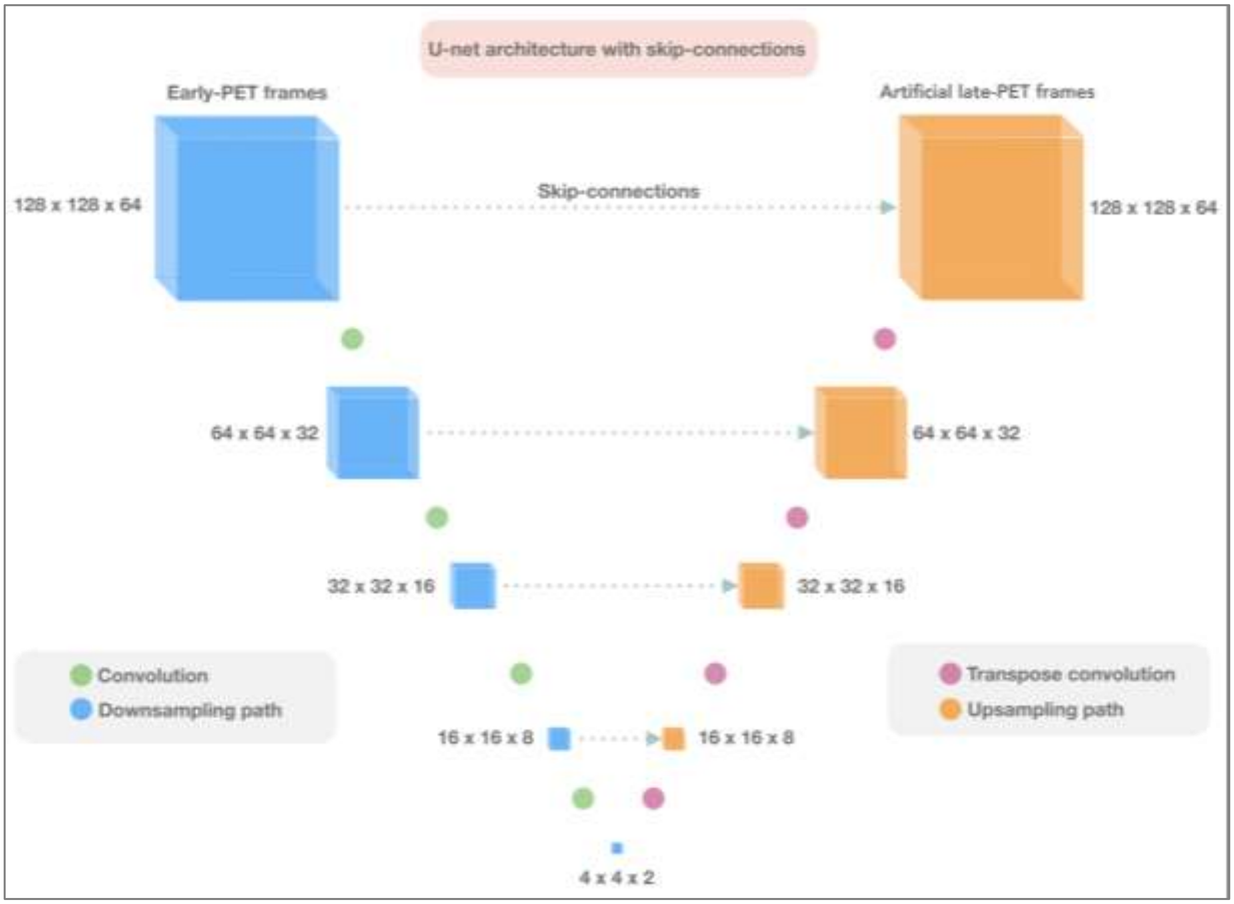

Supplemental Figure 1. Schematic representation of the 3D U-net generator architecture. The blue cubes correspond to a progressive down-sampling path, while the orange cubes correspond to the step-wise up-sampling path. The skip-connections are represented by dotted arrows and enable the preservation of high-frequency information.

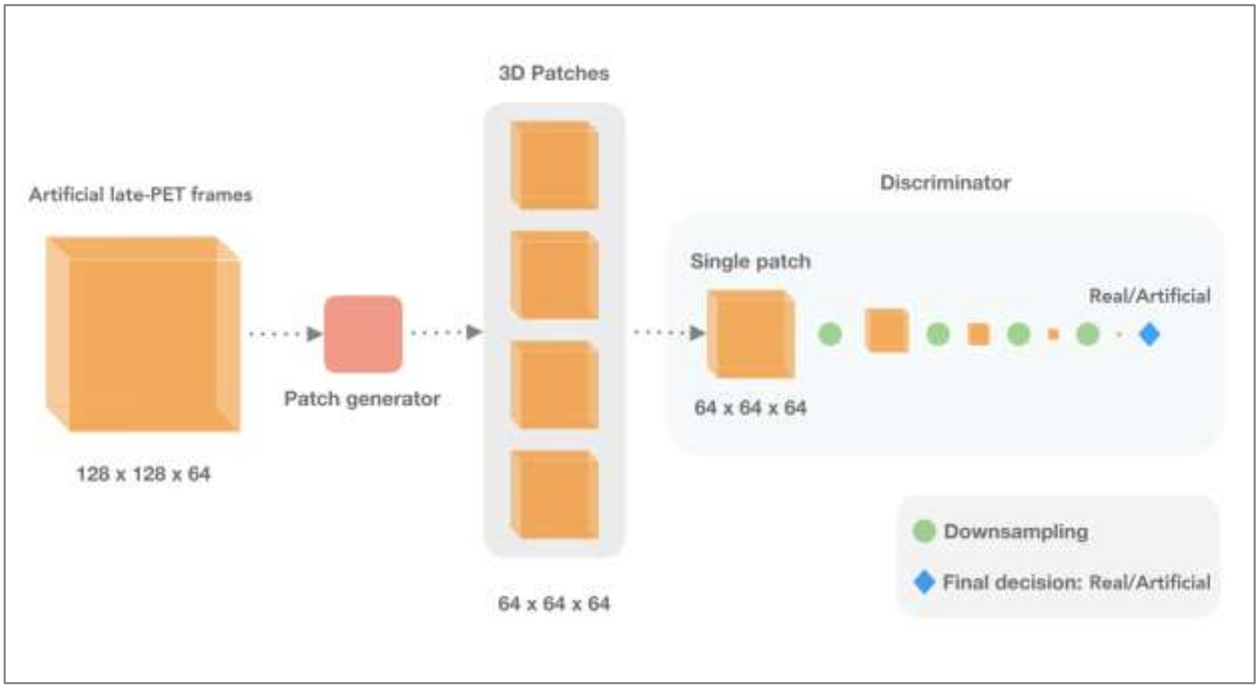

Supplemental Figure 2. Schematic representation of the patchGAN discriminator architecture. The inputs to the discriminator were patches of size 64 x 64 x 64 of the generator's output. The architecture consisted of 5 convolutional layers. The first down-sample layer produced 64 feature maps; this number was doubled at each subsequent down-sampling step. After the last layer, a convolution was applied to map to a 1-dimensional output, followed by a sigmoid activation to determine whether the input is a “real” full-dose PET image or an “artificial” image.

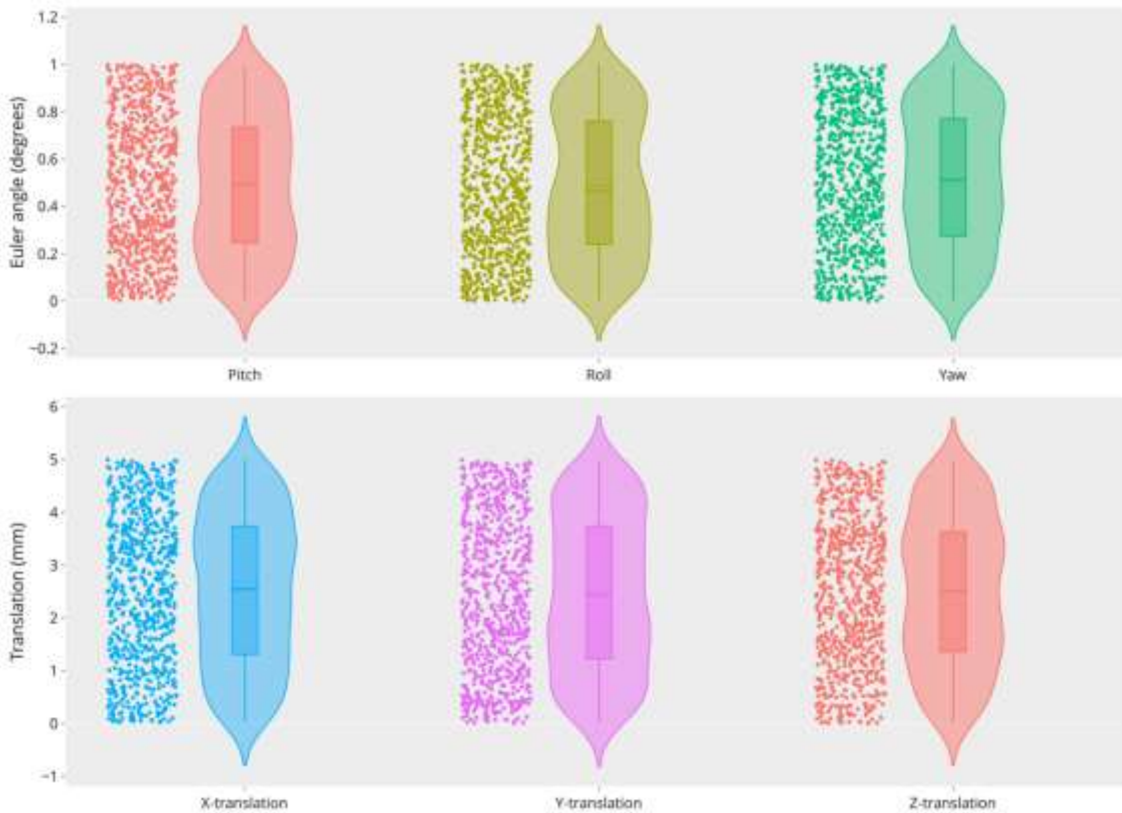

Supplemental Figure 3. Distribution of the motion parameters (rotation and translation), which were used to create synthetically generated data sets that included additional motion. The rotational parameters varied between 0 to 1 degree in all 3 orientations, and the translational parameters varied between 0 mm to 5 mm in x-, y- and z-directions.

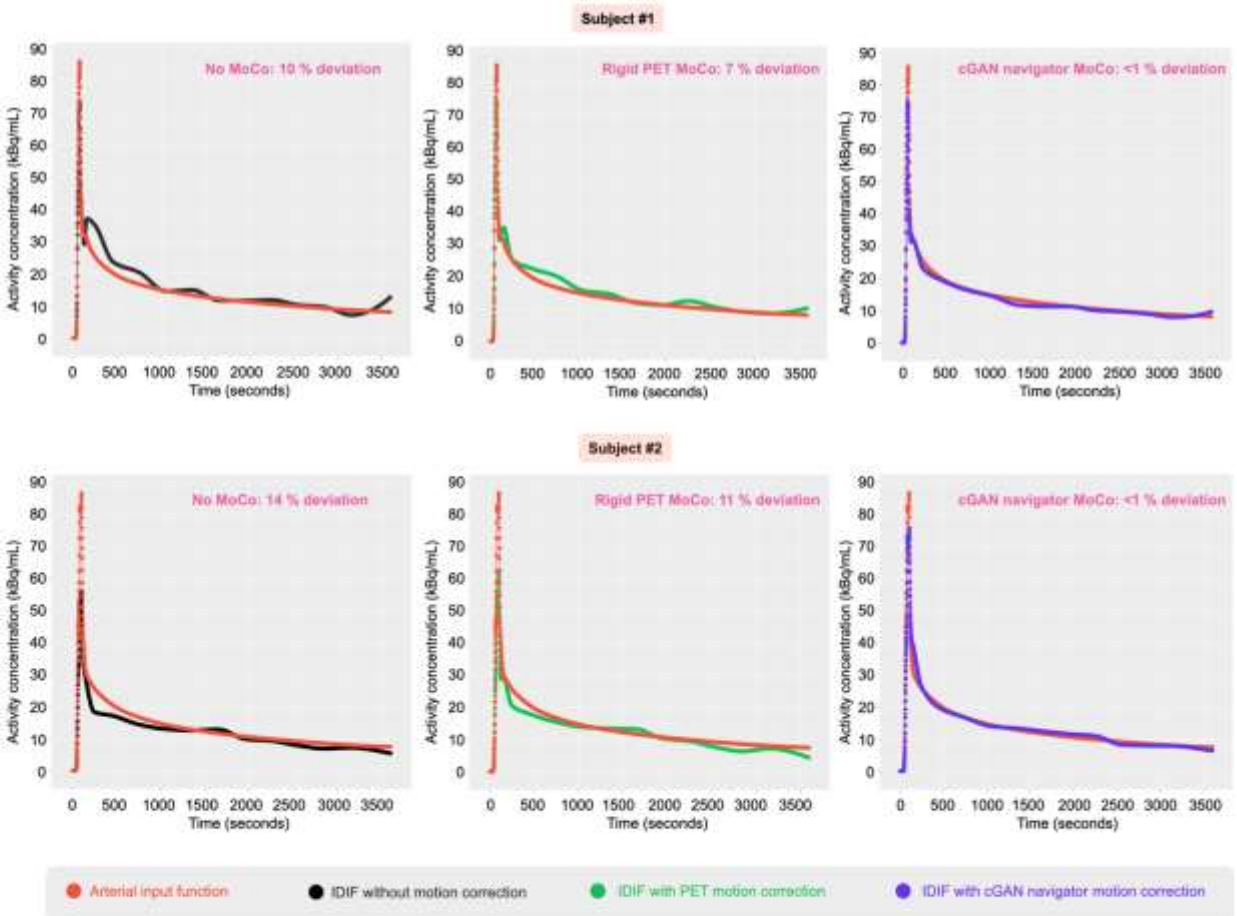

Supplemental Figure 4**.** Representative input functions derived from two test subjects (#1 and #2) demonstrating the ability of cGAN processing to yield an accurate IDIF. Substantial motion artefacts were present in the early stages of the study (0 – 15min p.i., black time-activity curve) as determined by comparison with the reference standard of arterial blood sampling (orange time-activity curve). Application of frame-based motion correction results in an improved, but still suboptimal time-activity curves (green). cGAN-aided motion correction allows the non-invasive extraction of an IDIF (blue) that closely reproduces arterial blood samples.

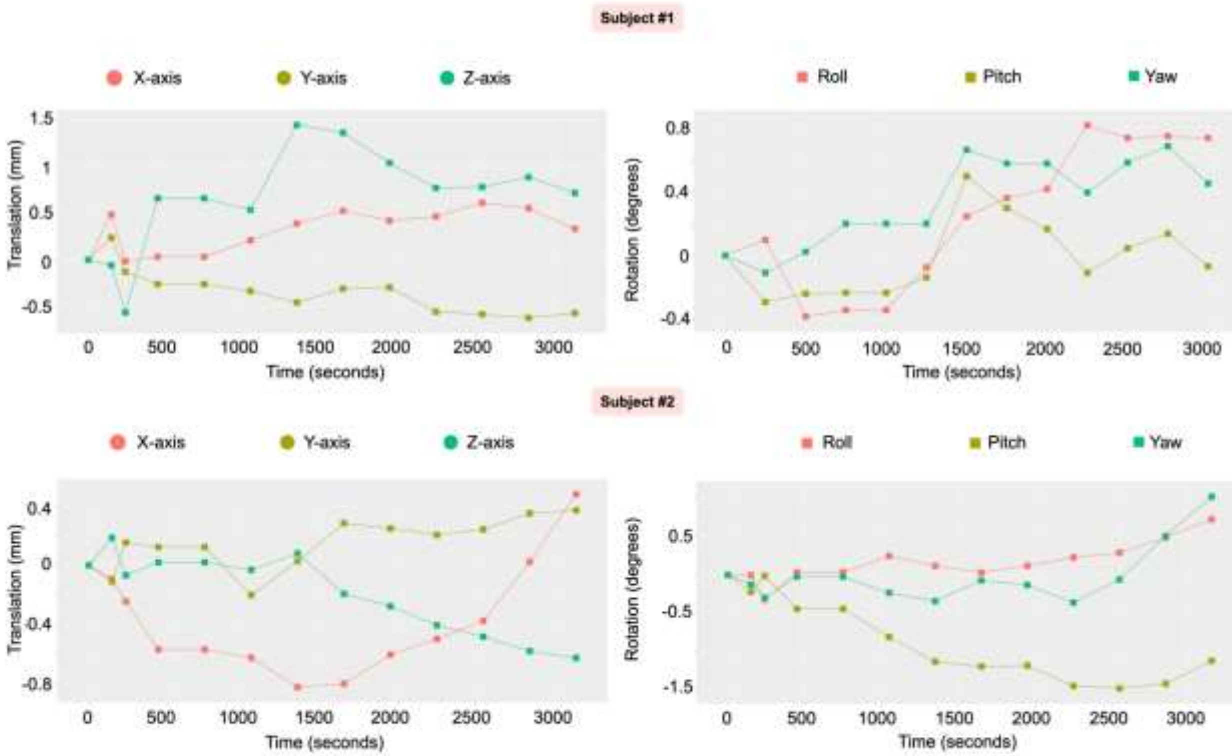

Supplemental Figure 5. 3D motion profile (3 translation and 3 rotation parameters) of representative subjects #1 and #2 from whom a non-invasive IDIF was derived (see also Suppl Fig 4).

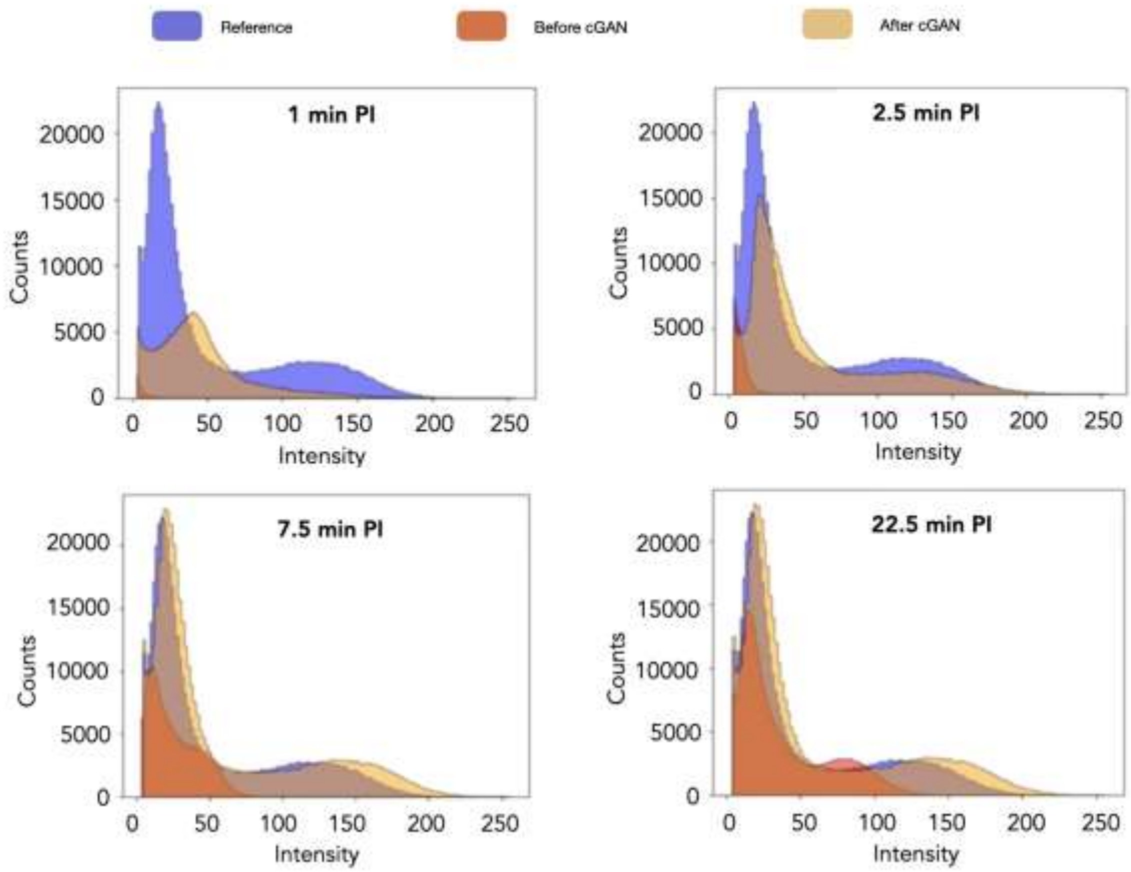

Supplemental Figure 6. Comparison of the reference image histograms (blue) with the histogram of the low-count original image prior to cGAN (orange) and post cGAN (yellow) processing. It can be seen that in the cGAN processed histogram the frequency of high intensities in the image is overestimated (7.5 min p.i and 22.5 min p.i).

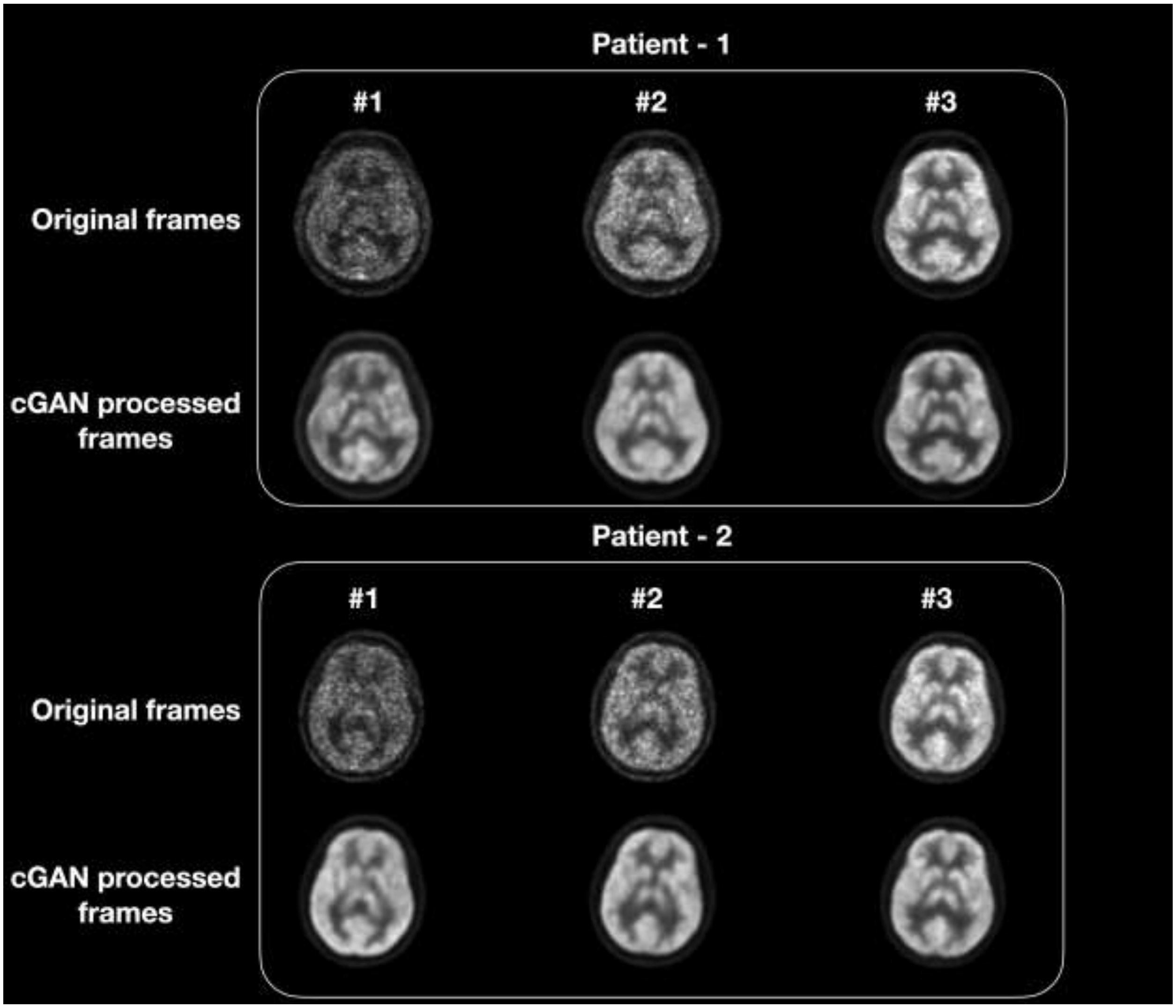

Supplemental Figure 7. The mappings (M-n) trained using 18F-FDG dynamic datasets from the Siemens Biograph mMR was applied to the dynamic datasets (2 scans) obtained from an external PET/CT system. Frames 1, 2 and 3 correspond to the following PET mid-times (2, 7, 35 min p.i). Although cGAN mappings were trained using data from the on-site PET/MR system, they were able to produce reasonable results with data obtained from an external PET/CT system, supporting the claim that cGAN mappings might be useable across imaging systems.